CRYSTAL GROWTH & DESIGN

Article

Improving the Performance of Planar Perovskite Solar Cells through Pre-heated, Delaying Annealing Process to Control Nucleation and Phase Transition of Perovskite Films

Hui Liu, Hairui Liu, Jien Yang, Feng Yang, Zhiyong Liu, and Sagar M. Jain

Cryst. Growth Des., **Just Accepted Manuscript** • DOI: 10.1021/acs.cgd.9b00024 • Publication Date (Web): 10 Jun 2019

is published by the American Chemical Society. 1155 Sixteenth Street N.W., Washington, DC 20036

Improving the Performance of Planar Perovskite Solar Cells through Pre-heated, Delaying Annealing Process to Control Nucleation and Phase Transition of Perovskite Films

Hui Liu[1], Hairui Liu[1*], Jien Yang[1], Feng Yang[1], Zhiyong Liu[1] and Sagar M. Jain[2*]

1. College of Physics & Materials science, Henan Normal University, Henan Key Laboratory of Photovoltaic Materials, Xinxiang 453007, PR China.

2. SPECIFIC, College of Engineering, Swansea University Bay Campus, Fabian Way, SA1 8EN Swansea, United Kingdom.

Email i.d. of corresponding author

Hairui Liu – liuhuilh14@126.com

Sagar M. Jain – s.m.jain@swansea.ac.uk , sagarmjain@gmail.com

Abstract

Obtaining good quality perovskite absorber film remains a challenging task that limits performance of planar perovskite solar cells. . In this work, we demonstrated the importance of pre-heating treatment on perovskite nucleation and phase transition. . Fine-tuning the appropriate pre-heating and standing time resulted in the formation of high quality perovskite films with enhanced optoelectronic properties.. Pre-heated perovskite films with delaying of 1 hour post-annealing achieved the hysteresis-free, record power conversion efficiency (PCE) of 16.18%. While the perovskite films without preheating treatment in solar cells shown only12.35% efficiency.. This improved performance with pre-heating treatment and delay annealing of perovskite films found as a result of homogeneous nucleation and formation of high quality perovskite films. Improved perovskite quality is further evidenced from enhanced optoelectronic and crystalline properties of the perovskite absorber after preheating treatment.

1. Introduction

Organic-inorganic hybrid perovskite solar cells (PSCs) emerged as the potential candidate for next-generation photovoltaic technology and have drawn much attention as a result of low-cost fabrication and high performance.[1-3] In recent years, the power conversion efficiency (PCE) for PSCs has been raised remarkably from 3.8 % in 2009 to a certified 24.2 % in 2019.[4, 5] In a regular planar-heterojunction PSC, perovskite absorber layer of high crystalline quality are important for device performance.[6,7] Because the optoelectronic properties of PSCs depends on morphology, crystalline quality and coverage of the perovskite films.[8] After the deposition of the precursor materials, usually a (thermal) annealing step is necessary, which can convert the deposited precursors into the desired high-quality, crystalline perovskite phase.[7,9,11]

Thermal annealing step is the key parameter defining quality of perovskite absorber film. [9,10] Compare to the conventional mesoporous perovskite solar cells, PSCs with inverted solar cell architecture is close to commercialization and easy to fabricate on flexible substrates due to low temperature processing.[7-11] However, it is quite challenging task to obtain good quality perovskite films. Particularly, when deposited on hole transport PEDOT:PSS (Poly(3,4-ethylenedioxythiophene)-poly(styrenesulfonate) substrate.[7-10] This is due to the – hydrophilic and acidic nature of PEDOT:PSS that makes perovskite film formation difficult. Therefore, various methods have been adopted by scientific community to enhance the nucleation and crystal growth of perovskite films in planar architecture solar cells. For instance, applying external-electric-field and vacuum during annealing process for planar PSCs to assist crystallization,[12,13] employing gas-assisted solution technique during the spin coating to change the nucleation kinetics[14,15] and incorporating additives or solvents in precursor solution to facilitate homogeneous nucleation growth.[16, 17]

In this study we demonstrated that modifying the conventional thermal treatment have potential to tune the morphology and crystallization of perovskite to achieve a favorable morphology and improved crystal quality. Many research group experienced, that precursor films when subjected to stand for minutes before annealing yield better morphology and performance. Snaith's group left the spin-coating films in the glove box at room temperature for 30 minutes before annealing that assisted in controlling the perovskite morphology.[10] Wang et al. reported Pb-In precursor films were dried at room temperature about 20 minutes and obtained improved solar cell performance.[18] You

et al, used delay annealing process for inorganic $CsPbI_3$ perovskite absorber and obtained improved performance.. Delaying in annealing slows down the evaporation rate of the solvent to obtain a stable α-phase $CsPbI_3$.[19] Recently, Fan and co-workers treated the CuSCN films with conventional delaying in annealing treatment to get high quality hole transporting layers in PSCs.[20] Albertus and Jia et al. investigated the relation between device performance and delaying annealing approach in hybrid mesoscopic/planar perovskite solar cells by one-step and two-step methods, respectively.[21, 22] However, the reason why delaying in annealing is beneficial to obtain good quality perovskite films is yet unknown. Moreover, the low-viscosity perovskite precursor solution can also lead to the formation of colloidal aggregates that makes the nucleation growth pathways during waiting process quite complicated.[23] It is timely and essential to investigate the growth pathways for perovskite crystallization under different thermal treatment process to fine tune the crystallization process in order to obtain high quality perovskite films. in for planar PSCs.

In this direction, we fabricated PEDOT:PSS based inverted PSCs by adding pre-heating process and appropriate standing time during conventional annealing process. $CH_3NH_3PbI_xCl_{3-x}$ absorber layer is employed by one step spin coating deposition procedure. For delay-annealing process, in order to promote nuclei growth, the films treated with 60°C for 10 minutes, the process of nucleation and phase transition were evidenced from the morphological and X-Ray diffraction measurements. Then, the films were subjected to different standing time as a waiting period. The detailed formation mechanism of $CH_3NH_3PbI_xCl_{3-x}$ absorber layer when subjected to different standing time is investigated systematically. The devices prepared with variable pre-heated delaying annealing treatment were found to have improved efficiency over devices prepared with conventional annealing process. A record PCE of 16.18% is obtained for perovskite film with pre-heated standing time of 1 hour.

2. EXPERIMENTAL SECTION

2.1 Materials preparation

All materials were purchased from Xi'an polymer light technology corporation, China (https://p-oled.lookchem.com/). To prepare the $CH_3NH_3PbI_xCl_{3-x}$ () perovskite precursor solution. MAI and $PbCl_2$ were dissolved in 1 ml of N,N-dimethylformamide (DMF, 99.8%) in a 3:1 molar ratio. 20 mg of $PC_{61}BM$ was dissolved in 1 ml of chlorobenzene. Bphen (4,7-Diphenyl-1,10-

phenanthroline) was dissolved in absolute ethanol with the concentration of 0.6 mg/ml. PEDOT:PSS was blend with isopropanol in a 20:1 volume ratio. All the solutions mentioned above were stirred at 60 ℃ overnight except PEDOT:PSS, which is sonicated at 0 ℃ for 15 minutes and all of the above were filtered with 0.45 μm nylon filters before device fabrication.

2.2 Device fabrication

Solar devices were fabricated in the configuration of ITO/PEDOT:PSS/$MAPbI_xCl_{3-x}$/$PC_{61}BM$/Bphen/Ag. Indium doped tin oxide (15 Ω/sq) glass substrates cleaned with detergent, deionized water, acetone and ethanol respectively and undergone sonication for 20 minutes at 40 ℃. After being air dried, the substrates were further treated with ultraviolet-ozone (UV-Ozone) treatment for 15 minutes. Then PEDOT:PSS solution was deposited by spin-coating at 4500 rpm for 40 seconds and annealed at 140 ℃ for 30 minutes in air. After cooling down, the substrates were transferred into a nitrogen filled glove box. Perovskite precursor solution was then spin-coated on the PEDOT:PSS at 4000 rpm for 40 s. The fabrication processes for the perovskite layers treated with different thermal treatment techniques is illustrated in Scheme 1. For the conventional annealing method (Scheme 1(a)), the obtained $MAPbI_xCl_{3-x}$ precursor films were subjected to conventional annealing process. In conventional annealing process, the films were slowly heated from 60 ℃ to 100 ℃ at a rate of 10 ℃/10 minutes for 90 minutes. While, in the delaying of annealing process (Scheme 1(b)), the films after spin-coating allowed to standing for a certain time and then continued the gradient annealing process as mentioned above. For the pre-heated delaying annealing method (Scheme 1(c)), the precursor films were firstly pre-heated at 60 ℃ for 10 minutes, then cooled to ambient temperature. These films were placed in a petri dish at room temperature in the glove box for standing time of 0.5, 1, 2.5, 5, 7.5 and 10 hours respectively. After waiting time, the gradient annealing process is employed to finalize the crystal growth and eliminate or minimize the by-product formation. The electron-transporting layer $PC_{61}BM$ (Phenyl-C61-butyric acid ester) and Bphen (4,7-Diphenyl-1,10-phenanthroline) interfacial layer deposited by spin coating speed of 2000 rpm for 40 seconds. Finally, the samples are transferred to a vacuum chamber for silver metal electrode deposition under high vacuum through a shadow mask having a device area of 6.25 mm^2.

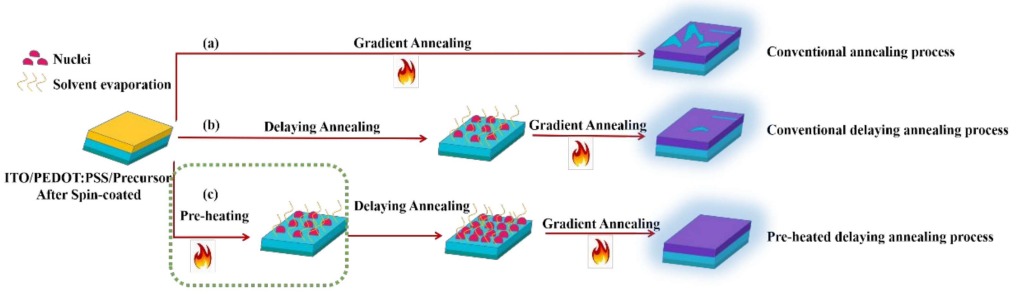

Scheme 1. Schematic illustration of perovskite absorber layers treated with (a) conventional annealing process, (b) conventional delaying annealing process, and (c) pre-heated delaying annealing process, respectively.

2.3 Characterization and Measurement

X-ray diffraction (XRD) data was collected on Panalytical X'Pert pro X-ray powder diffractometer with Cu Kα radiation (λ=0.154 nm). The absorption spectra of the perovskite films measured on a Varian 5E UV/vis/NIR spectrophotometer. Scanning electron microscopy (SEM) were performed with field-emission electrons using Nova 230 Nano SEM. Axioplan microscope (ZEISS) was used for measuring optical microscope images. To determine the perovskite film coverage from SEM images, A greyscale threshold was used to define perovskite was distinct from the substrate, and percentage coverage was then calculated by the software program.

The Current-voltage and dark current measurements performed using (2400 Series Source Meter, Keithley Instruments) under simulated Air-Mass (AM) 1.5 sunlight at 100 mW/cm^2 (Newport, Class AAA solar simulator, 94023A-U). The external quantum efficiency (EQE) measurements were performed using a system combining a Xenon lamp, a monochromator, a chopper and a lock-in amplifier together with a calibrated silicon photodetector.

3. Results and Discussion

3.1 Characterization of the Films Treated with Pre-heated Delaying Annealing Process

The surface morphology of the perovskite films was characterized by scanning electron microscopy (SEM) and the film coverage rates are calculated by the image analysis software ImageJ,[24] as shown in Figure 1. For the perovskite absorber films with conventional annealing process, large pinholes observed (Fig.1(a)), and the calculated coverage of the perovskite film is only 91%. Hence, the exposed ITO/PEDOT:PSS surface on the film form contact between the electron and hole transporting layers, which mightact as the shunting pathway that is detrimental

for the device performance.[11] Prolonged standing time to 1 hour results into the formation of densely connected perovskite films with high surface coverage and larger grain size. Strikingly, the surface coverage rate of the film reached to around 98% (Fig.2(c)), implying that high quality films with large crystal grains (Fig. 1(c)) have formed with less surface defects.[8] Compared with the reference (perovskite films prepared with conventional annealing), larger perovskite grains appeared in the films with standing time of 1 hour, indicating the formation of enhanced quality perovskite films. Further prolonging standing time to 2.5 and 5 hours (Fig.1(d) and (e) respectively), leading to the appearance of pronounced cracks in the perovskite films and as a result surface coverage gradually decreased. On increasing the standing time to 7.5 and 10 hours, the perovskite film coverage decreased further (Fig.S1(a)) deteriorating the quality of the perovskite films. Thus the desired quality of perovskite films can be easily fine-tuned by controlling the delaying annealing time.

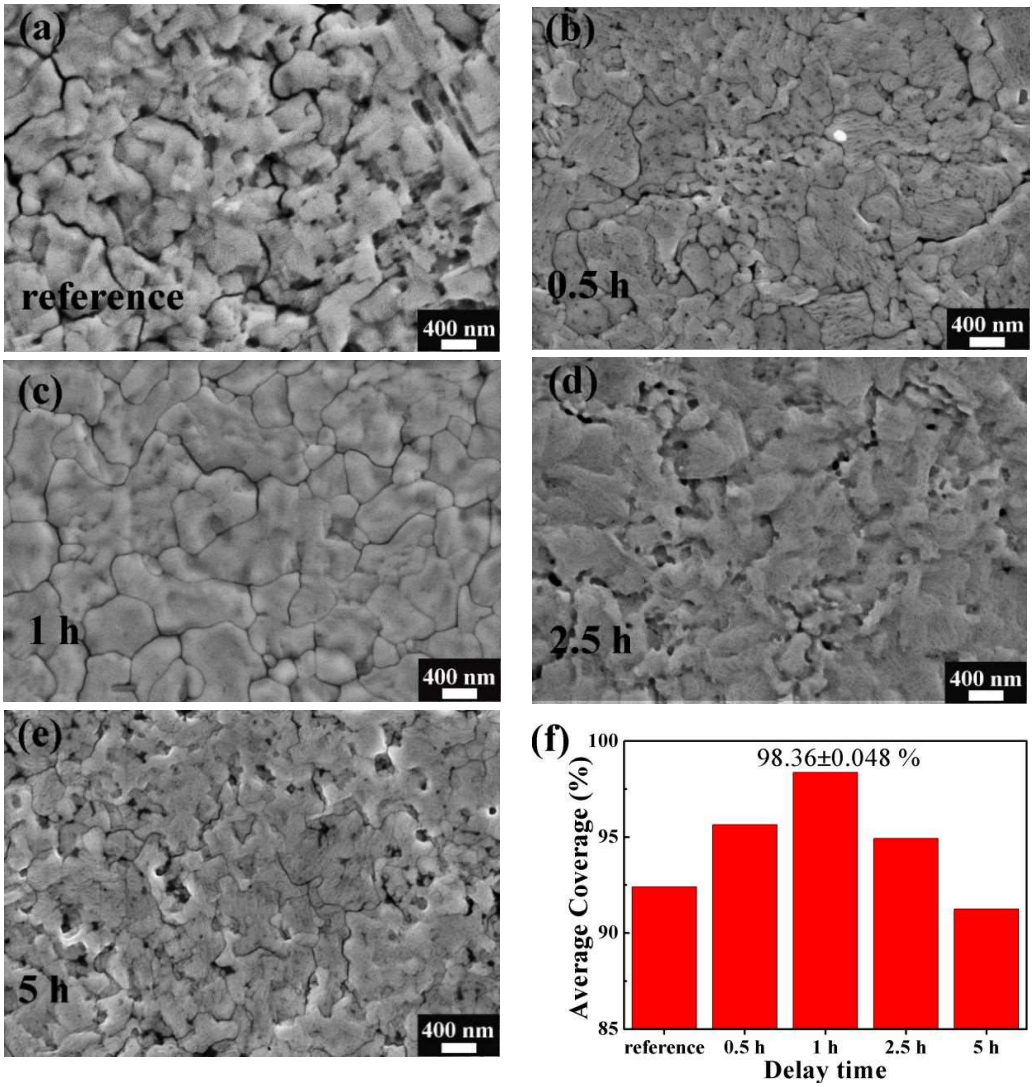

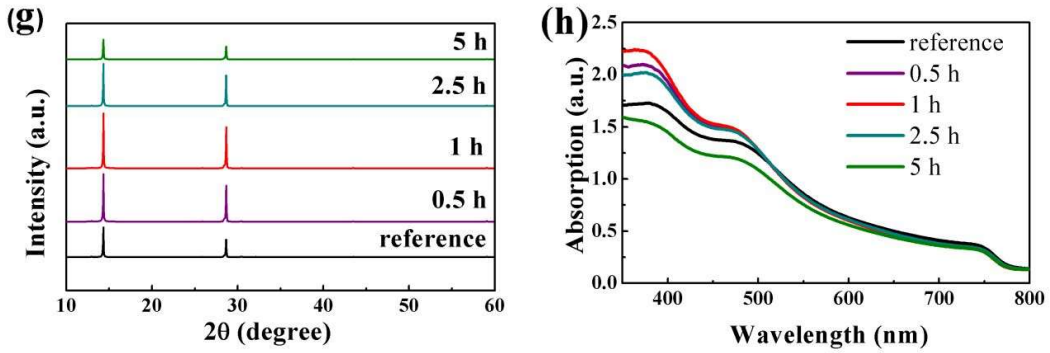

Figure 1. (a) Top-view scanning electron microscopy (SEM) images of the final film treated with conventional gradient annealing, (b)-(e) are SEM images of the final pre-heated films with different delaying annealing time. (f) Average perovskite surface coverage of corresponding SEM images (a-e) calculated by ImageJ software based on three measurement per data point. (g) X-ray diffraction spectrum and (h) UV-Visible absorption spectra of perovskite films with corresponding delay annealing time treatment.

To investigate the influence of delay annealing time on crystallinity and crystal structure of the related perovskite films, X-ray diffraction (XRD) pattern of the perovskite films with variable pre-heated delaying annealing time were measured and the results shown in Fig.1 (g). All the perovskite films display two distinct diffraction peaks located at 14.2° and 28.4° assigned to the (110) and (220) crystal planes of the tetragonal phase of perovskite.[25] With the standing time increasing from 0 to 5 hours, the intensities of diffraction peaks are significantly enhanced until 1 hour standing time after this time the crystalline quality shows a steady drop. This observation indicates that delaying annealing has substantial influence on the purity and crystallization of the perovskite films. The X-ray diffraction peak intensity steadily increases with standing time to 7.5 and 10 hours. As presented in Fig.S1(c). The change of crystallization might be related to improved volatilization of dimethyl formamide (DMF) during the standing process. As delay annealing process allows more time for DMF vapors providing a wet environment that the precursor ions and molecules diffuse a long distance in the film than that treated with conventional annealing.[26, 27]

The morphology and crystallinity of perovskite absorber film significantly influences optical properties and ultimately the performance of PSCs. Fig.1 (h) presents the UV-visible absorption spectrum of pre-heated films with variable delaying annealing time. All of spectra exhibit the typical perovskite absorption spectra with a sharp absorption onset at 800 nm. It can be found that

absorption coefficient firstly increased and then decreased in the shorter wavelength region with the increasing of delaying annealing time and achieved the highest value for absorber films with 1 hour standing time before annealing, which was attributed to the improved crystallinity of the films.[28] As shown in Fig. S1(d), the absorption intensity improved again with the standing time increasing from 7.5 to 10 hours, which can be attributed to the better crystallization, bigger grain sizes, fewer pinholes and higher coverage of perovskite films.[29] The XRD results shows the same trend. The films treated with pre-heated delaying of 1 hour to annealing possess excellent crystallization and absorption properties.[27] In summary, pre-heating and proper standing time is highly convenient to fine-tune the nucleation velocity, crystal growth process and film morphology of perovskite absorber.[11, 30]

3.2 The Significance of Pre-heating Process

Fabrication of excellent quality perovskite film rely on homogeneous distribution of nucleation centers, annealing temperature and vapor evaporation atmosphere.[31, 32] Hence, it is critical to control the growth of crystal nuclei.

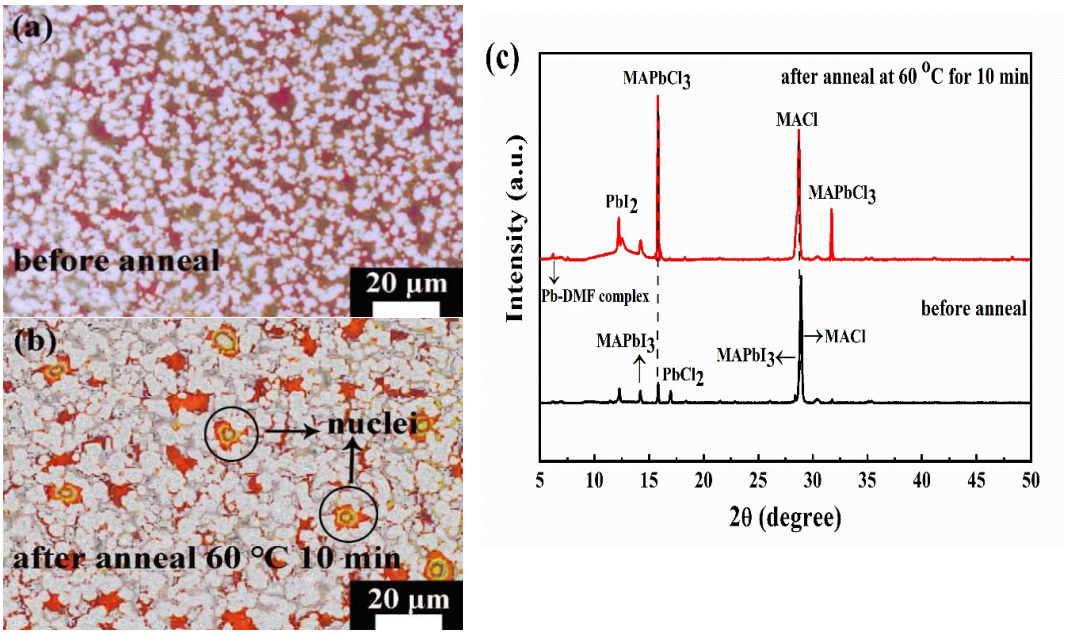

Figure 2. Optical microscopy images (a-b) and XRD spectrum (c) of perovskite films with initial stage before and after pre-heated at 60 ℃ for 10 minutes.

Fig. 2 shows the optical microscopy images and XRD pattern for the perovskite films before and after pre-heating treatment at 60 ℃ for 10 minutes. Fig. 2 (a) corresponds to the sample treated

with the conventional delaying annealing process at the early stage of nucleation (before annealing), it is clearly visible that there are no crystal nuclei exist on the film, but once the sample is subjected to anneal at 60 ℃ for 10 minutes, small number of crystal nuclei emerged on the surface of the film represented in circles in Fig. 2 (b). For the sample without pre-heating, there was not enough time and suitable temperature to evaporate DMF to form $[PbI_6]^{4-}$ cage. Hence, crystal nuclei not appeared in the film.[33] While for the conventional annealing process, the film with spin-coated precursor solution were annealed on the hot plate at once, this accelerate the evaporation of DMF and directs random crystal growth in all directions. For the conventional delay annealing process, crystal nuclei forms on substrate in irregular fashion. But pre-heated process would provide thermal gradient support (suitable temperature) for nuclei to grow at early stage. Thus assisting the formation of high-quality perovskite films.

Fig.2 (c) shows XRD peaks at 28.7° can be observed for the sample with pre-heated treatment (annealed at 60 ℃ for 10 minutes), which can attributed to the MACl.[34] Small intensity diffraction peaks at 12.2°, 14.2°, 15.8° and 16.9° appears, which are signature of PbI_2 (001), $MAPbI_3$ (110),[35-37] $MAPbCl_3$ (100),[38] and $PbCl_2$ phase[34] respectively. For the perovskite films after pre-heated treatment, the new peaks at 6.2° appeared, the peak represents the intermediate Pb-DMF complex.[35-37] For the perovskite films annealed at 60 ℃ for 10 minutes, diffraction peaks at 15.8° and 31.7° shown substantial improvement. (20 times) representing the (100) and (200) cubic crystal structure peaks for $MAPbCl_3$.[38] The peak intensity at 12.2° indexed to PbI_2 shows substantial growth indicating increased amount of crystalline PbI_2. On contrary, the peak at 16.9° representing $PbCl_2$ is disappeared.

From X-ray diffraction measurements and previous reported studies on $CH_3NH_3PbI_xCl_{3-x}$ phase transformation.[34,39-43] We propose following reaction (1)

$$PbCl_2 + 3MAI \rightarrow MAPbI_3 + 2MACl\uparrow (MA: CH_3NH_3^+) \quad \text{.....(1)}$$

Small amount of PbI_2 phase is observed for the sample without pre-heated treatment. This is surprising and possibly due to the room temperature ion exchange between $PbCl_2$ and MAIas presented in Equ.(2). Moreover, we can observe other crystalline phases clearly in the X-ray diffraction pattern of the film without annealing treatment this indicates standing time can provide sufficient energy for phase formation. Successive post annealing accelerated DMF evaporation,

resulting in formation of intermediate Pb-DMF complex. The already formed MACl and PbI_2 react with $PbCl_2$ and MAI to form $MAPbCl_3$ and $MAPbI_3$ (equation (3) and (4)). As the crystalline phase of $PbCl_2$ formation is higher than the PbI_2. this results into formation of $MAPbCl_3$ phase this can be clearly observed in X-Ray diffraction and shown in reaction (3). After pre-heated treatment, a significant $MAPbCl_3$ and PbI_2 appeared by consuming $PbCl_2$ which is completely disappeared. This indicates that the pre-heating promotes reaction (2) and (3). Some fraction of $PbCl_2$ may translate into PbI_2 by reaction (2), remaining fraction reacts with MACl to form $MAPbCl_3$. The absence of XRD peak at 28.4° for the sample with pre-heating might be related to the decomposition of $MAPbI_3$ (equ.(5)) during the pre-heating process.

$$PbCl_2 + 2\,MAI \rightleftharpoons PbI_2 + 2\,MACl\uparrow \quad \text{.....(2)}$$

$$PbCl_2 + MACl \rightleftharpoons MAPbCl_3 \quad \text{.....(3)}$$

$$PbI_2 + MAI \rightleftharpoons MAPbI_3 \quad \text{.....(4)}$$

$$MAPbI_3 \overset{\Delta}{\rightleftharpoons} PbI_2 + CH_2NH_2\uparrow + HI\uparrow \quad \text{.....(5)}$$

3.3 Growth Mechanism of Perovskite Film during Delaying in Annealing Process

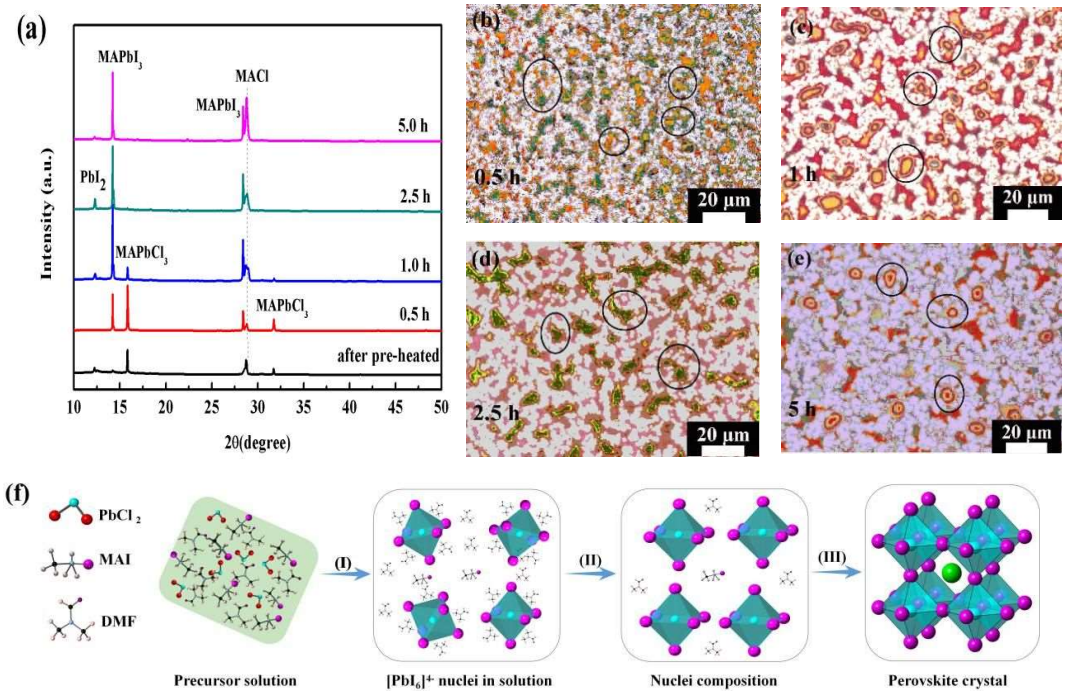

Figure 3. XRD spectrum (a) and optical microscopy images (b-e) of initial stage of perovskite nucleation with different standing time. (f) Schematic nano-assembly process of perovskite crystallization.

After pre-heated at 60 ℃ for 10 minutes, the perovskite films were treated with different standing time and the mechanism of the standing time influence the formation of high quality perovskite films were investigated systematically. Fig.3 displays XRD spectrum (a) and the optical microscopy images (b-e) of thermal treated perovskite films with different standing time. (f) is the Nano-assemble model of the perovskites from the pristine precursor solution to perovskite crystals.

As observed from X-ray diffraction Fig.3 (a) of perovskite films treated with delaying different time to anneal after pre-heated treatment, perovskite mainly composed by cubic phase $MAPbCl_3$, and accompanied by tetragonal phase $MAPbI_3$ (XRD peaks at 14.2° and 28.4°) and crystalline MACl exists at 28.9°. For the sample with standing time of 0.5 hours, the peak intensity of tetragonal phase $MAPbI_3$ and $MAPbCl_3$ significantly enhanced. On prolonged standing time to 1 hour, the diffraction peak of $MAPbI_3$ further improved intensity. However, the peak intensity of $MAPbCl_3$ reduced. It is observed from X-ray diffraction measurements that the perovskite films formed employing delaying annealing yields high crystalline characteristics and good coverage as a result of controlling the evaporation of solution and phase transition during delaying annealing process. Optical microscopy is employed to monitor the surface of perovskite films. The results showed in Fig.3. Interestingly, the sample with standing time 0.5 hour (Fig.3(b))shows irregularly distributed flower-like shaped nuclei gradually emerged from the substrate. The magnified optical microscopy image shown in Fig. S2.[11, 44] Further prolonging standing time to 1 hour, results in the formation of the big spherical crystals, uniformly distributed on the surface of the substrate (Fig.3(c)) showing formation of a dense perovskite films. Further increasing the standing time upto 2.5 hours (Fig.3(d)), nuclei became more larger and shows more homogeneous distribution.[45-48] These results confirmed that the nucleation stage is well controlled by delaying annealing process. Which determines the final morphology of the perovskite films. The number of nuclei shown obvious decrease when the standing time increased to 5 and 10 hours (Fig.S3(a) and (b)). This is an indication that the nuclei have grown into bigger crystalline grains.[49, 50]

These results confirmed that delaying annealing process not just affects the formation process of nucleation but homogeneous growth of perovskite crystals, this is because this process offers the nuclei enough time and space to adjust themselves to adopt the equilibrium condition of homogeneous distribution required for smooth and better quality of perovskite films. Also it is reported that $CH_3NH_3^+$ rich environment can slow down the perovskite formation process and thus

improve the growth of the crystal domains.[34] Besides, the evaporation of DMF promote the growth of crystal along the grain boundary. So, larger perovskite grains and less grain boundaries appears for perovskite film.

The transformation of pristine precursor solution into perovskite polycrystals is described by following three nano-assemble steps: (Ⅰ) After spin coating precursor solution, the sample is pre-heated at 60 ℃ for 10 minutes resulting into formation of $[PbI_6]^{4-}$ cage. $[PbI_6]^{4-}$ octahedron surrounded with MAI and DMF solvent by electrostatic forces (Fig. 3(f)). (Ⅱ) Variable standing time after pre-heating provides enough time for the solvent evaporation to decrease the inter-cage distance for $[PbI_6]$.[33] (Ⅲ) After post fine-tuning the standing time, it is required to continue with conventional gradient annealing process (second annealing) to eliminate the by-products and to get the high quality perovskite crystals.

3.4 Device Performance

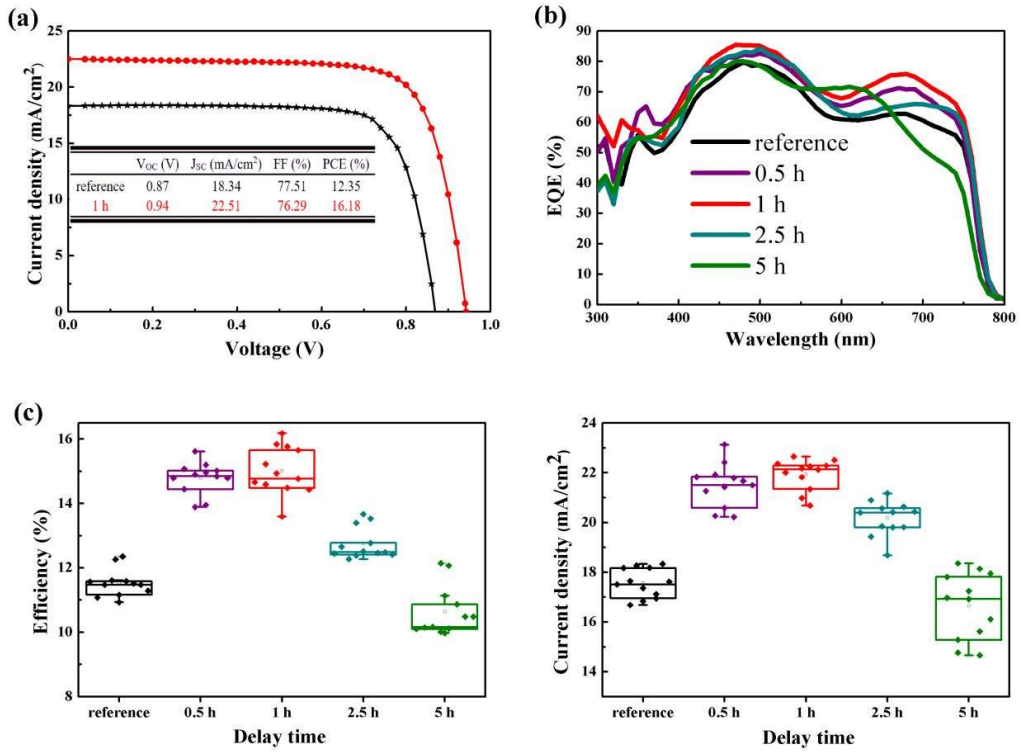

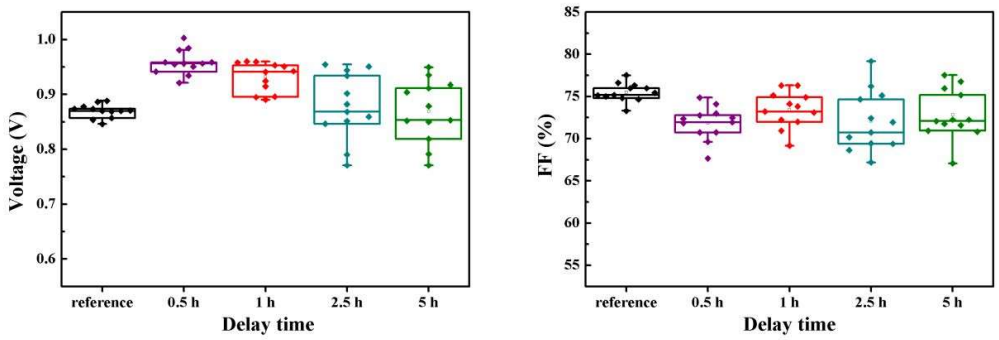

Figure 4. (a) Current density-voltage (J-V) curves of the reference devices and the devices of absorber films treated with pre-heated delaying 1 hour to anneal, which under AM 1.5 solar illumination to measure. (b) External quantum efficiency (EQE) spectrum of the cells. (c) The box diagrams of devices parameters, the corresponding absorber layers treated with pre-heated, variable delaying annealing time. Cell size: 6.25 mm^2.

As observed from the X-ray diffraction, UV-visible characterization and further proved from enhanced device efficiency, the formation of nuclei and the quality of perovskite films were impacted remarkably by pre-heating and delaying annealing process. Thus, the relationship between photovoltaic performance of PSCs and corresponding perovskite films with pre-heated delaying different annealing time is studied. Fig.4(a) shows the current density-voltage (J-V) curves of champion PSCs assembled with the perovskite absorber films treated with conventional annealing process (reference device) and pre-heated delaying 1 hour to anneal, which were measured by reverse bias scan under 1 sun AM 1.5 G illumination. The optimized device with standing time of 1 hour yeild a highest record PCE of 16.18% (*Jsc* = 22.5 mA/cm^2, *Voc* = 0.94 V and Fill factor = 76.3%). External quantum efficiency (EQE) spectrum of the respective films (Figure 4(b)) shows that the PSCs prepared with delay annealing perovskite films for 1 hour shows highest coverage reaching maximum at 85% of the EQE spectrum.

For all devices, EQE reached a peak value at ≈480 nm with a gradual decrease from 500 to 580 nm. There is no large difference between 0 and 5 hours among 300−500 nm. However, the sample with delaying 5 hours to anneal showed a remarkable decrease at 600−800 nm, indicating a photocurrent loss due to either decrease in the absorption of perovskite layer or possible optical interference.[35] Devices prepared from the perovskite absorber films of increased standing time, the EQE spectrum coverage reached maximum at 1 hour standing time and then further increasing

standing time decreased the EQE coverage. Perovskite films with standing time for 1 hour achieved the highest values and shown a broad plateau over 80 % between 400 and 750 nm wavelength verifying excellent photoelectric conversion characteristics.

The photovoltaic parameters, open-circuit voltage (V_{OC}), short-circuit current density (J_{SC}), fill factor (*FF*) and PCE of 12 devices with different standing time are shown in Fig. 4(c) and corresponding photovoltaic parameters are summarized in Table S1. Devices prepared with absorber layer of delaying annealing time shows improved current density (J_{SC}) until delay time reaches 1 hour further prolonging delay in annealing shows drop in current density. The same trend is shown for open-circuit voltage. With the optimized standing time of 1 hour, the efficiency of PSCs substantially raised from 12.35% (reference devices) to 16.18%. The improved performance is directly related to the good coverage, high crystalline quality. Devices with high quality absorber films would effectively decrease charge carrier trapping rate.[27,29, 51, 52] Dark current measurement were carried out to characterize the recombination of free carriers and charge carrier loss, as displayed in Fig.S4.The improvement in open-circuit voltage is due to the reduced defect-induced recombination in the devices.[53, 54].

The perovskite devices prepared from absorber layer of prolonged standing time of 2.5 to 5 hours shown gradual drop in efficiency. The performance of device with film delaying 2.5 hours to anneal dropped mainly since the formation of PbI_2 as well the intermediate phases increased rapidly While perovskite phase decreased during the waiting period which passivate the grain boundaries and usually worked as recombination centers.[8, 35, 37] However, the performance dropped substantially for the devices with absorber films having standing time of 7.5 hours (Fig.S5(a) and (b)), this can be explained by the fact that the intensity of $MAPbCl_3$ raised again since 7.5 hours (Fig.S3(c)), clarifying that mentioned phases during the waiting period also influenced the intensity of final perovskite film and the related device performance enormously. It is widely reported that $MAPbI_xCl_{3-x}$ films hold the same characteristic XRD peaks as the $MAPbI_3$ films. Hence the specific compound can not to be identified.[55-58] We believe that the variable ratio of Cl/I among the films formed as a result of variable delaying annealing time have significant effect on photovoltaic performance.

The devices with pre-heated delaying annealing time of 1 hour exhibited the best PCE values. We observed that pre-heating and delaying annealing process are advantageous to improve the

device performance. Especially, for large scale production delaying annealing time need to be considered as one of the crucial parameters to control the quality of perovskite films.

4. Conclusions

In summary, we have discussed the necessity of pre-heating process before conventional delaying annealing to fine tune the nuclei growth , promote homogeneous nucleation and for obtaining high quality $MAPbCl_3$ films. Fine-tuning the delaying annealing time after pre-heated treatment. facilitate homogeneous nucleation and improve the optoelectronic quality of the perovskite films. Planar perovskite solar cells prepared with optimized delay annealing of 1 hour resulted into champion performance with highest PCE of 16.18%. This is significant improvement in performance as compared to the devices (12.35%) prepared with conventional annealing treatment. The finding of this work specially the pre-heated delaying annealing process that shown enhanced optoelectronic and crystalline properties of perovskite films is promising to extend the improvement in the performance of other mixed cation perovskite solar cells as well for development of highly sensitive large scale fabrication of perovskite solar cells.

Supporting Information. cg-2019-00024d.R2 contain the supplementary data for this paper.

The following files are available free of charge. Additional details of Scanning electron microscope images, XRD patterns, UV-visible spectra, optical microscopy, current-voltage density curves, and histogram of device parameters in table as well figures (PDF)

AUTHOR INFORMATION

Corresponding Authors

Hairui Liu* liuhairui1@126.com

Sagar M. Jain* s.m.jain@swansea.ac.uk; sagarmjain@gmail.com

Notes

The authors declare no competing financial interest.

Supporting information is available, listing the contents of the material supplied as supporting information.

ACKNOWLEDGMENTS

This work was supported by the National Natural Science Foundation of China (No: 51502081 and 11747069). Science and Technique Program of Henan Province (No. 182102210375). Author S. M. J. is thankful to Welsh assembly Government funded Sêr Cymru Solar project, EPSRC grants EP/M025020/1 (Supergen Solar Challenge) and Marie-Curie COFUND fellowship for financial support. European Union's Horizon 2020 research and innovation programme under the Marie Skłodowska-Curie grant agreement No 663830.

References

(1) Tan, H.; Jain, A.; Voznyy, O.; Lan, X.; Fp, G. D. A.; Fan, J. Z.; Quintero-Bermudez, R.; Yuan, M.; Zhang, B.; Zhao, Y., Efficient and Stable Solution-Processed Planar Perovskite Solar Cells via Contact Passivation. *Science* **2017,** 355, 722-726.

(2) Stranks, S. D.; Eperon, G. E.; Grancini, G.; Menelaou, C.; Alcocer, M. J.; Leijtens, T.; Herz, L. M.; Petrozza, A.; Snaith, H. J., Electron-Hole Diffusion Lengths Exceeding 1 Micrometer in an Organometal Trihalide Perovskite Absorber. *Science* **2013,** 342, 341-344.

(3) Peng, J.; Sun, Y.; Chen, Y.; Yao, Y.; Liang, Z., Light and Thermally Induced Evolutional Charge Transport in $CH_3NH_3PbI_3$ Perovskite Solar Cells. *ACS Energy Lett.* **2016,** 1, 1000-1006.

(4) https://www.nrel.gov/pv/cell-efficiency.html.

(5) Jeon, N. J.; Na, H.; Jung, E. H.; Yang, T.-Y.; Lee, Y. G.; Kim, G.; Shin, H.-W.; Il Seok, S.; Lee, J.; Seo, J., A Fluorene-Terminated Hole-Transporting Material for Highly Efficient and Stable Perovskite Solar Cells. *Nat. Energy* **2018,** 3, 682-689.

(6) Bi, C.; Wang, Q.; Shao, Y.; Yuan, Y.; Xiao, Z.; Huang, J., Non-Wetting Surface-Driven High-Aspect-Ratio Crystalline Grain Growth for Efficient Hybrid Perovskite Solar Cells. *Nat. Comm.* **2015,** 6, 7747-7754.

(7) Ren, Y.-K.; Ding, X.-H.; Wu, Y.-H.; Zhu, J.; Hayat, T.; Alsaedi, A.; Xu, Y.-F.; Li, Z.-Q.; Yang, S.-F.; Dai, S.-Y., Temperature-Assisted Rapid Nucleation: a Facile Method to Optimize the Film Morphology for Perovskite Solar Cells. *J. Mater. Chem. A* **2017,** 5, 20327-20333.

(8) Song, T.-B.; Chen, Q.; Zhou, H.; Luo, S.; Yang, Y.; You, J.; Yang, Y., Unraveling Film Transformations and Device Performance of Planar Perovskite Solar Cells. *Nano Energy* **2015,** 12, 494-500.

(9) Zhu, L.; Shi, J.; Lv, S.; Yang, Y.; Xu, X.; Xu, Y.; Xiao, J.; Wu, H.; Luo, Y.; Li, D.; Meng, Q., Temperature-Assisted Controlling Morphology and Charge Transport Property for Highly Efficient Perovskite Solar Cells. *Nano Energy* **2015,** 15, 540-548.

(10) Eperon, G. E.; Burlakov, V. M.; Docampo, P.; Goriely, A.; Snaith, H. J., Morphological Control for High Performance, Solution-Processed Planar Heterojunction Perovskite Solar Cells. *Adv. Funct. Mater.* **2014,** 24, 151-157.

(11) Song, S.; Hörantner, M. T.; Choi, K.; Snaith, H. J.; Park, T., Inducing Swift Nucleation Morphology Control for Efficient Planar Perovskite Solar Cells by Hot-Air Quenching. *J. Mater. Chem. A* **2017,** 5, 3812-3818.

(12) Zhang, C.-C.; Wang, Z.-K.; Li, M.; Liu, Z.-Y.; Yang, J.-E.; Yang, Y.-G.; Gao, X.-Y.; Ma, H., Electric-Field Assisted Perovskite Crystallization for High-Performance Solar Cells. *J. Mater. Chem. A* **2018,** 6, 1161-1170.

(13) Xian, X. F.; Di, Z.; Huimin, S.; Xingang, R.; Kam Sing, W.; Michael, G. T.; Choy, W. C. H., Vacuum-Assisted Thermal Annealing of $CH_3NH_3PbI_3$ for Highly Stable and Efficient Perovskite Solar Cells. *ACS Nano* **2015,** 9, 639-646.

(14) Huang, F.; Dkhissi, Y.; Huang, W.; Xiao, M.; Benesperi, I.; Rubanov, S.; Zhu, Y.; Lin, X.; Jiang, L.; Zhou, Y., Gas-Assisted Preparation of Lead Iodide Perovskite Films Consisting of a Monolayer of Single Crystalline Grains for High Efficiency Planar Solar Cells. *Nano Energy* **2014,** 10, 10-18.

(15) Chiang, C. H.; Wu, C. G., A Method for the Preparation of Highly Oriented $MAPbI_3$ Crystallites for High-Efficiency Perovskite Solar Cells to Achieve an 86% Fill Factor. *ACS Nano* **2018,** 12, 10355-10364.

(16) Liang, P. W.; Liao, C. Y.; Chueh, C. C.; Zuo, F.; Williams, S. T.; Xin, X. K.; Lin, J.; Jen, A. K., Additive Enhanced Crystallization of Solution-Processed Perovskite for Highly Efficient Planar-Heterojunction Solar Cells. *Adv. Mater.* **2014,** 26, 3748-3754.

(17) Shen, D.; Yu, X.; Cai, X.; Peng, M.; Ma, Y.; Su, X.; Xiao, L.; Zou, D., Understanding the Solvent-Assisted Crystallization Mechanism Inherent in Efficient Organic–Inorganic Halide Perovskite Solar Cells. *J. Mater. Chem. A* **2014,** 2, 20454-20461.

(18) Wang, Z. K.; Li, M.; Yang, Y. G.; Hu, Y.; Ma, H.; Gao, X. Y.; Liao, L. S., High Efficiency Pb-In Binary Metal Perovskite Solar Cells. *Adv. Mater.* **2016,** 28, 6695-6703.

(19) Wang, P.; Zhang, X.; Zhou, Y.; Jiang, Q.; Ye, Q.; Chu, Z.; Li, X.; Yang, X.; Yin, Z.; You, J., Solvent-Controlled Growth of Inorganic Perovskite Films in Dry Environment for Efficient and Stable Solar Cells. *Nat. Commum.* **2018,** 9, 2225-2232.

(20) Fan, L.; Li, Y.; Yao, X.; Ding, Y.; Zhao, S.; Shi, B.; Wei, C.; Zhang, D.; Li, B.; Wang, G.; Zhao, Y.; Zhang, X., Delayed Annealing Treatment for High-Quality CuSCN: Exploring Its Impact on Bifacial Semitransparent n-i-p Planar Perovskite Solar Cells. *ACS Appl. Energy Mater.* **2018,** 1, 1575-1584.

(21) Sutanto, A. A.; Lan, S.; Cheng, C.-F.; Mane, S. B.; Wu, H.-P.; Leonardus, M.; Xie, M.-Y.; Yeh, S.-C.; Tseng, C.-W.; Chen, C.-T.; Diau, E. W.-G.; Hung, C.-H., Solvent-Assisted Crystallization via a Delayed-Annealing Approach for Highly Efficient Hybrid Mesoscopic/Planar Perovskite Solar Cells. *Sol. Energy Mat. Sol. C.* **2017,** 172, 270-276.

(22) Jia, F.; Guo, Y.; Che, L.; Liu, Z.; Zeng, Z.; Cai, C., Synergic Solventing-Out Crystallization with Subsequent Time-Delay Thermal Annealing of PbI_2 Precursor in Mesostructured Perovskite Solar Cells. *Mater. Res. Express* **2018,** 5, 066404-066417.

(23) Yan, K.; Long, M.; Zhang, T.; Wei, Z.; Chen, H.; Yang, S.; Xu, J., Hybrid Halide Perovskite Solar Cell Precursors: Colloidal Chemistry and Coordination Engineering Behind Device Processing for High Efficiency. *J. Am. Chem. Soc.* **2015,** 137, 4460-4468.

(24) Schneider, C. A.; Rasband, W. S.; Eliceiri, K. W., NIH Image to ImageJ: 25 Years of Image Analysis. *Nat. Methods* **2012,** 9, 671-676.

(25) Conings, B.; Baeten, L.; De Dobbelaere, C.; D'Haen, J.; Manca, J.; Boyen, H. G., Perovskite-Based Hybrid Solar Cells Exceeding 10% Efficiency with High Reproducibility Using a Thin Film Sandwich Approach. *Adv. Mater.* **2014,** 26, 2041-2046.

(26) Xiao, Z.; Dong, Q.; Bi, C.; Shao, Y.; Yuan, Y.; Huang, J., Solvent Annealing of Perovskite-Induced Crystal Growth for Photovoltaic-Device Efficiency Enhancement. *Adv. Mater.* **2014,** 26, 6503-6509.

(27) Li, L.; Zhang, F.; Hao, Y.; Sun, Q.; Li, Z.; Wang, H.; Cui, Y.; Zhu, F., High Efficiency Planar Sn–Pb Binary Perovskite Solar Cells: Controlled Growth of Large Grains Via a One-Step Solution Fabrication Process. *J. Mater. Chem. C* **2017,** 5, 2360-2367.

(28) Yang, M.; Zhang, T.; Schulz, P.; Li, Z.; Li, G.; Kim, D. H.; Guo, N.; Berry, J. J.; Zhu, K.; Zhao, Y., Facile Fabrication of Large-Grain $CH_3NH_3PbI_{3-x}Br_x$ Films for High-Efficiency Solar Cells Via CH_3NH_3Br-Selective Ostwald Ripening. *Nat. Commun.* **2016,** 7, 12305-12314.

(29) Ma, Y.; Liu, Y.; Shin, I.; Hwang, I. W.; Jung, Y. K.; Jeong, J. H.; Park, S. H.; Kim, K. H., Understanding and Tailoring Grain Growth of Lead-Halide Perovskite for Solar Cell Application. *ACS Appl. Mater. Interfaces* **2017,** 9, 33925-33933.

(30) Raga, S. R.; Jung, M.-C.; Lee, M. V.; Leyden, M. R.; Kato, Y.; Qi, Y., Influence of Air Annealing on High Efficiency Planar Structure Perovskite Solar Cells. *Chem. Mater.* **2015,** 27, 1597-1603.

(31) Zhao, Y.; Zhu, K., Organic-Inorganic Hybrid Lead Halide Perovskites for Optoelectronic and Electronic Applications. *Chem. Soc. Rev.* **2016,** 45, 655-689.

(32) Huang, F.; Pascoe, A. R.; Wu, W. Q.; Ku, Z.; Peng, Y.; Zhong, J.; Caruso, R. A.; Cheng, Y. B., Effect of the Microstructure of the Functional Layers on the Efficiency of Perovskite Solar Cells. *Adv. Mater.* **2017,** 29, 1601715-1601725.

(33) Hu, Q.; Zhao, L.; Wu, J.; Gao, K.; Luo, D.; Jiang, Y.; Zhang, Z.; Zhu, C.; Schaible, E.; Hexemer, A.; Wang, C.; Liu, Y.; Zhang, W.; Gratzel, M.; Liu, F.; Russell, T. P.; Zhu, R.; Gong, Q., In Situ Dynamic Observations of Perovskite Crystallisation and Microstructure Evolution Intermediated from $[PbI_6]^{(4-)}$ Cage Nanoparticles. *Nat. Commun.* **2017,** 8, 15688-15697.

(34) Yu, H.; Wang, F.; Xie, F.; Li, W.; Chen, J.; Zhao, N., The Role of Chlorine in the Formation Process of "$CH_3NH_3PbI_{3-x}Cl_x$" Perovskite. *Adv. Funct. Mater.* **2014**, 7102-7108.

(35) Zhou, H.; Chen, Q.; Li, G.; Luo, S.; Song, T. B.; Duan, H. S.; Hong, Z.; You, J.; Liu, Y.; Yang, Y., Interface Engineering of Highly Efficient Perovskite Solar Cells. *Science* **2014,** 345, 542-546.

(36) Burschka, J.; Pellet, N.; Moon, S. J.; Humphry-Baker, R.; Gao, P.; Nazeeruddin, M. K.; Gratzel, M., Sequential Deposition as a Route to High-Performance Perovskite-Sensitized Solar Cells. *Nature* **2013,** 499, 316-319.

(37) Supasai, T.; Rujisamphan, N.; Ullrich, K.; Chemseddine, A.; Dittrich, T., Formation of a Passivating $CH_3NH_3PbI_3/PbI_2$ Interface During Moderate Heating of $CH_3NH_3PbI_3$ layers. *Appl. Phys. Lett.* **2013,** 103, 183906-183910.

(38) Liu, Y.; Yang, Z.; Cui, D.; Ren, X.; Sun, J.; Liu, X.; Zhang, J.; Wei, Q.; Fan, H.; Yu, F.; Zhang, X.; Zhao, C.; Liu, S. F., Two-Inch-Sized Perovskite $CH_3NH_3PbX_3$ (X = Cl, Br, I) Crystals: Growth and Characterization. *Adv. Mater.* **2015,** 27, 5176-5183.

(39) Dualeh, A.; Gao, P.; Seok, S. I.; Nazeeruddin, M. K.; Grätzel, M., Thermal Behavior of Methylammonium Lead-Trihalide Perovskite Photovoltaic Light Harvesters. *Chem. Mater.* **2014,** 26, 6160-6164.

(40) Wang, S.; Jiang, Y.; Juarez-Perez, E. J.; Ono, L. K.; Qi, Y., Accelerated Degradation of Methylammonium Lead Iodide Perovskites Induced by Exposure to Iodine Vapour. *Nat. Energy* **2016,** 2, 16195-16204.

(41) Dualeh, A.; Tétreault, N.; Moehl, T.; Gao, P.; Nazeeruddin, M. K.; Grätzel, M., Effect of Annealing Temperature on Film Morphology of Organic-Inorganic Hybrid Pervoskite Solid-State Solar Cells. *Adv. Funct. Mater.* **2014,** 24, 3250-3258.

(42) Fan, L.; Ding, Y.; Luo, J.; Shi, B.; Yao, X.; Wei, C.; Zhang, D.; Wang, G.; Sheng, Y.; Chen, Y.; Hagfeldt, A.; Zhao, Y.; Zhang, X., Elucidating the Role of Chlorine in Perovskite Solar Cells. *J. Mater. Chem. A* **2017,** 5, 7423-7432.

(43) Jain, S.M.; Philippe, B.; Johansson, E.; Park, B.W.; Hakan, R.; Edvinsson, T. and Boschloo, G., Vapor Phase Conversion of PbI_2 to $CH_3NH_3PbI_3$: Spectroscopic Evidence for Formation of an Intermediate Phase. J. Mater. Chem. A **2016**, 4, 2630-2642.

(44) Xiao, M.; Huang, F.; Huang, W.; Dkhissi, Y.; Zhu, Y.; Etheridge, J.; Gray-Weale, A.; Bach, U.; Cheng, Y.-B.; Spiccia, L., A Fast Deposition-Crystallization Procedure for Highly Efficient Lead Iodide Perovskite Thin-Film Solar Cells. *Angew. Chem. Int. Ed.* **2014,** 53, 9898-9903.

(45) Banfield, J. F.; Welch, S. A.; Zhang, H.; Ebert, T. T.; Penn, R. L., Aggregation-Based Crystal Growth and Microstructure Development in Natural Iron Oxyhydroxide Biomineralization Products. *Science* **2000,** 289, 751-754.

(46) Bogush, G. H.; Iv, C. F. Z., Uniform Silica Particle Precipitation: An Aggregative Growth Model. *J. Colloid Interf. Sci.* **1991,** 142, 19-34.

(47) Johnson, N. J.; Korinek, A.; Dong, C.; van Veggel, F. C., Self-Focusing by Ostwald Ripening: a Strategy for Layer-By-Layer Epitaxial Growth on Upconverting Nanocrystals. *J. Am. Chem. Soc.* **2012,** 134, 11068-11071.

(48) Chen, Y.; Johnson, E.; Peng, X., Formation of Monodisperse and Shape-Controlled MnO Nanocrystals in Non-Injection Synthesis: Self-Focusing Via Ripening. *J. Am. Chem. Soc.* **2007,** 129, 10937-10947.

(49) Shtukenberg, A. G.; Punin, Y. O.; Gujral, A.; Kahr, B., Growth Actuated Bending and Twisting of Single Crystals. *Angew. Chem. Int. Ed. Engl.* **2014,** 53, 672-699.

(50) Jain, S.M.; Qiu,Z.; Haggman, L.; Mirmohades, M.; Johansson, M.B.; Edvinsson, T.; Boschloo, G., Frustrated Lewis Pair-Mediated Recrystallization of $CH_3NH_3PbI_3$ for Improved Optoelectronic Quality and High Voltage Planar Perovskite Solar Cells. Energy Environ. Sci. **2016**, 9, 3770-3782.

(51) Green, M. A.; Ho-Baillie, A.; Snaith, H. J., The Emergence of Perovskite Solar Cells. *Nat. Photo.* **2014,** 8, 506-514.

(52) Lin, Q.; Armin, A.; Burn, P. L.; Meredith, P., Organohalide Perovskites for Solar Energy Conversion. *Acc. Chem. Res.* **2016,** 49, 545-553.

(53) Zhu, H. L.; Xiao, J.; Mao, J.; Zhang, H.; Zhao, Y.; Choy, W. C. H., Controllable Crystallization of $CH_3NH_3Sn_{0.25}Pb_{0.75}I_3$ Perovskites for Hysteresis-Free Solar Cells with Efficiency Reaching 15.2%. *Adv. Funct. Mater.* **2017,** 27, 1605469-1605477.

(54) You, J.; Hong, Z.; Yang, Y.; Chen, Q.; Cai, M.; Song, T. B.; Chen, C. C.; Lu, S.; Liu, Y.; Zhou, H., Low-Temperature Solution-Processed Perovskite Solar Cells with High Efficiency and Flexibility. *ACS Nano* **2014,** 8, 1674-1680.

(55) Samu, G. F.; Janáky, C.; Kamat, P. V., A Victim of Halide Ion Segregation. How Light Soaking Affects Solar Cell Performance of Mixed Halide Lead Perovskites. *ACS Energy Lett.* **2017,** 2, 1860-1861.

(56) Yoon, S. J.; Draguta, S.; Manser, J. S.; Sharia, O.; Schneider, W. F.; Kuno, M.; Kamat, P. V., Tracking Iodide and Bromide Ion Segregation in Mixed Halide Lead Perovskites during Photoirradiation. *ACS Energy Lett.* **2016,** 1, 290-296.

(57) Hoke, E. T.; Slotcavage, D. J.; Dohner, E. R.; Bowring, A. R.; Karunadasa, H. I.; McGehee, M. D., Reversible Photo-Induced Trap Formation in Mixed-Halide Hybrid Perovskites for Photovoltaics. *Chem. Sci.* **2015,** 6, 613-617.

(58) Hoffman, J. B.; Schleper, A. L.; Kamat, P. V., Transformation of Sintered $CsPbBr_3$ Nanocrystals to Cubic $CsPbI_3$ and Gradient $CsPbBr_xI_{3-x}$ through Halide Exchange. *J. Am. Chem. Soc.* **2016,** 138, 8603-8611.

For Table of Contents Use Only

Improving the Performance of Planar Perovskite Solar Cells through Pre-heated, Delaying Annealing Process to Control Nucleation and Phase Transition of Perovskite Films

Hui Liu[1], Hairui Liu[1*], Jien Yang[1], Feng Yang[1], Zhiyong Liu[1] and Sagar M. Jain[2*]

1. College of Physics & Materials science, Henan Normal University, Henan Key Laboratory of Photovoltaic Materials, Xinxiang 453007, PR China.

2. SPECIFIC, College of Engineering, Swansea University Bay Campus, Fabian Way, SA1 8EN Swansea, United Kingdom.

Email i.d. of corresponding author

Hairui Liu – liuhuilh14@126.com

Sagar M. Jain – s.m.jain@swansea.ac.uk , sagarmjain@gmail.com

TOC graphic

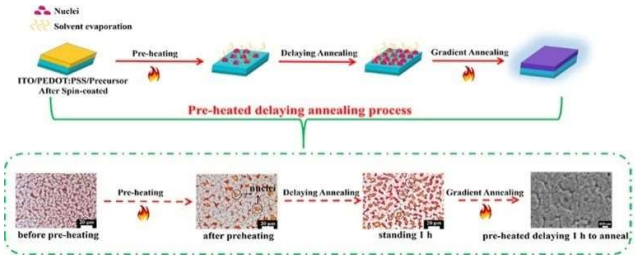

Synopsis

The necessity of pre-heating and the effect of delaying perovskite films annealing process on the quality of final films and devices performance were unraveled via crystallization and phase transition.